

## LETTERS

# Low-frequency earthquakes in Shikoku, Japan, and their relationship to episodic tremor and slip

David R. Shelly<sup>1</sup>, Gregory C. Beroza<sup>1</sup>, Satoshi Ide<sup>2</sup> & Sho Nakamura<sup>3</sup>

Non-volcanic seismic tremor was discovered in the Nankai trough subduction zone in southwest Japan<sup>1</sup> and subsequently identified in the Cascadia subduction zone<sup>2</sup>. In both locations, tremor is observed to coincide temporally with large, slow slip events on the plate interface downdip of the seismogenic zone<sup>2-7</sup>. The relationship between tremor and aseismic slip remains uncertain, however, largely owing to difficulty in constraining the source depth of tremor. In southwest Japan, a high quality borehole seismic network allows identification of coherent S-wave (and sometimes P-wave) arrivals within the tremor, whose sources are classified as low-frequency earthquakes. As low-frequency earthquakes comprise at

least a portion of tremor, understanding their mechanism is critical to understanding tremor as a whole. Here, we provide strong evidence that these earthquakes occur on the plate interface, coincident with the inferred zone of slow slip. The locations and characteristics of these events suggest that they are generated by shear slip during otherwise aseismic transients, rather than by fluid flow. High pore-fluid pressure in the immediate vicinity, as implied by our estimates of seismic P- and S-wave speeds, may act to promote this transient mode of failure. Low-frequency earthquakes could potentially contribute to seismic hazard forecasting by providing a new means to monitor slow slip at depth.

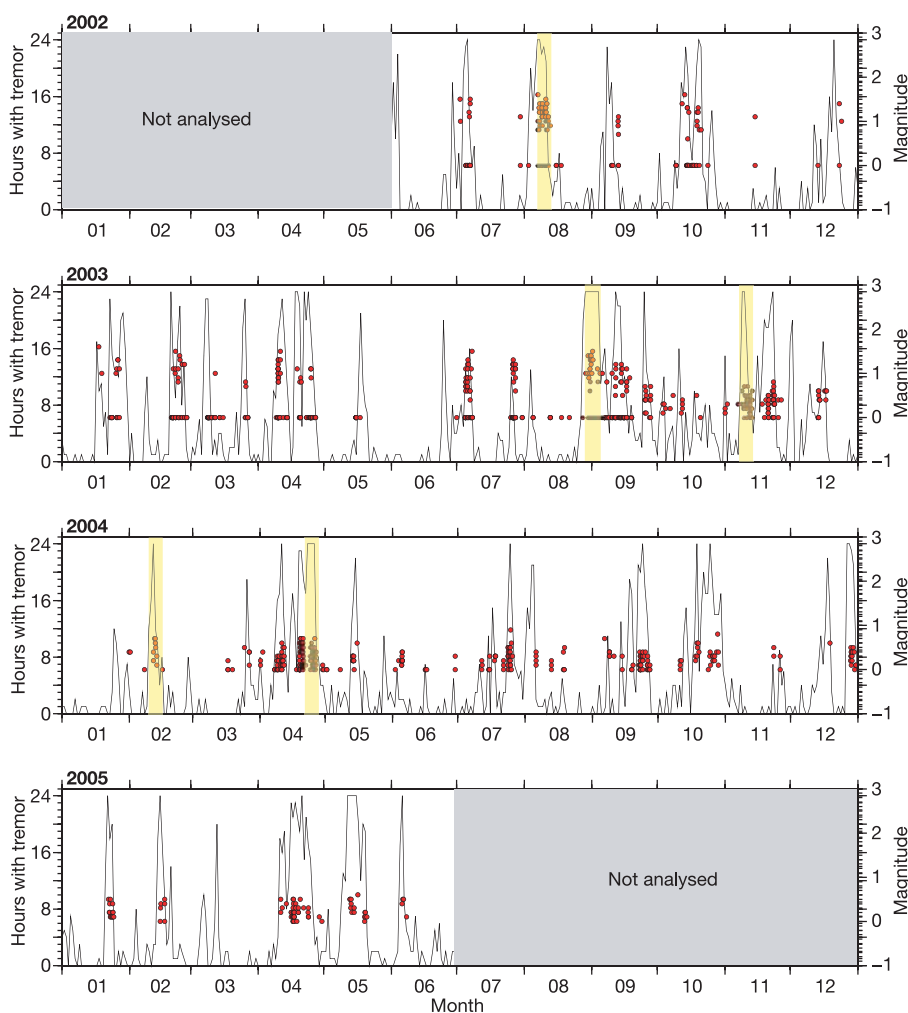


**Figure 1 | Comparison of temporal distribution of tremor activity and low-frequency earthquakes (LFEs) in western Shikoku.** The horizontal axis indicates time, with each year a separate panel, beginning in 2002. Red dots denote LFEs with magnitude on the vertical axis. The black line indicates the number of hours containing tremor per day. Yellow bars indicate the period and duration of detected slow slip events<sup>5,6</sup>, which are modelled to occur near the plate boundary beneath western Shikoku. Events with an undetermined magnitude are plotted as magnitude zero. The magnitude determination method changes during September 2003.

<sup>1</sup>Department of Geophysics, 397 Panama Mall, Stanford University, Stanford, California 94305-2215, USA. <sup>2</sup>Department of Earth and Planetary Science, University of Tokyo, Hongo 7-3-1, Bunkyo-ku, Tokyo 113-0033, Japan. <sup>3</sup>Earthquake Research Institute, University of Tokyo, Yayoi 1-1-1, Bunkyo-ku, Tokyo 113-0032, Japan.

A key to understanding the mechanism of deep non-volcanic tremor is determining exactly where it is generated; however, tremor is very difficult to locate owing to its small amplitude and the scarcity of coherent impulsive wave arrivals of the sort used to locate ordinary earthquakes. Epicentral locations based on seismogram envelope cross-correlation constrain tremor to lie within a belt that follows the strike of the subducting plate<sup>2</sup>. At these locations the depth of the plate interface is 30–45 km, but the depth of the tremor source is less certain.

At least two hypotheses might explain the observed tremor signals. One is that tremor is generated by the movement of fluids at depth, either by hydraulic fracturing<sup>1,8</sup> or by coupling between the rock and fluid flow<sup>9</sup>. In this model, tremor might be analogous to much shallower volcanic tremor, which is thought to arise from the coupling of fluid flow to the solid Earth in volcanic systems<sup>10,11</sup>. The correlation between tremor and aseismic slip could be explained if the slip is triggered by the same fluid movement that generates the tremor or, alternatively, if the fluid flow is a response to changes in stress and strain induced by slip<sup>12</sup>.

A second possibility is that tremor is generated directly by slow shear slip on the plate interface<sup>7</sup>. Under this hypothesis, tremor is the weak seismological signature of slip that is otherwise too slow to generate detectable seismic waves. In this scenario, tremor could be generated during aseismic transients as slip locally accelerates owing to the effects of geometric or physical irregularities on the plate interface. Fluids might play an auxiliary role, altering the conditions on the plate interface to enable transient slip events, without generating seismic waves directly.

Since 1999, the Japan Meteorological Agency (JMA) has differentiated a new class of events denoted as low-frequency earthquakes (LFEs) in their seismicity catalogue. These events occur almost exclusively as part of an extended duration tremor signal<sup>7,9</sup> (Fig. 1). They therefore correlate strongly with observed slow slip events. The LFEs and extended tremor also locate in approximately the same region<sup>1,6–9</sup> and exhibit similar migration behaviour along-strike<sup>1,5–7</sup>. Although it is uncertain whether or not LFEs and extended duration tremor represent a single phenomenon, their close association means that their mechanisms are probably intertwined. Figure 2 shows waveform records of a long-duration tremor sequence containing several LFEs. The visible arrivals from these events are primarily S waves, and if arrivals from the same source are distinguished at enough stations, the event is included in the JMA seismic catalogue. For such events, usually only the S-wave arrival time is reported. Owing to the lack of P-wave measurements and because the S-wave arrival is often emergent, catalogue locations of these events have large uncertainties, especially in depth.

To improve this situation, we use a combination of waveform cross-correlation and double-difference tomography<sup>13,14</sup> to relocate these LFEs in the western Shikoku region of the Nankai trough. We also obtain high-resolution velocity structure and precise locations of ordinary earthquakes. Although tremor (including LFEs) is observed along much of the Nankai trough, it is exceptionally active in western Shikoku.

Figure 3 shows the events, stations and the horizontal distribution of velocity inversion nodes used in this study. Vertically, the velocity node spacing is 5 km. In total, we relocate 6,713 events occurring between June 2002 and June 2005, including 1,180 LFEs, using waveforms from 112 seismic stations operated by the National Research Institute for Earth Science and Disaster Prevention (NIED), JMA, University of Tokyo and Kochi University. This includes 77 stations from the recently installed NIED Hi-net high-sensitivity borehole network, which provides especially high quality, low noise waveforms<sup>15</sup>. In addition to these data, we use P- and S-wave arrival time picks, provided by JMA for all stations. More details about the data and inversion process are included in Supplementary Information.

We find that the waveforms of LFEs recorded at the same station often correlate with each other, suggesting a similar source location

and mechanism for these events. Their waveform similarity is high enough for successful relocation using cross-correlation-derived differential times. Starting with only a rough estimate of the P- or S-wave arrival time, we obtain precise differential travel time measurements by cross-correlation waveform alignment. Supplementary Fig. S1 demonstrates the dramatic reduction in measurement error achieved by cross-correlation of LFE waveforms. Among the LFEs, S-wave correlations are particularly successful owing to the greater amplitude and signal to noise ratio of the S waves compared with P waves. However, despite the lack of P-wave arrival times in the catalogue, we are able to obtain P-wave differential arrival times for LFEs by correlating waveforms in a window centred on a theoretical P arrival time estimated from the S-wave arrival time and origin time (Supplementary Fig. S2). We are also able to obtain successful P-wave and S-wave correlations between some LFEs and ordinary earthquakes

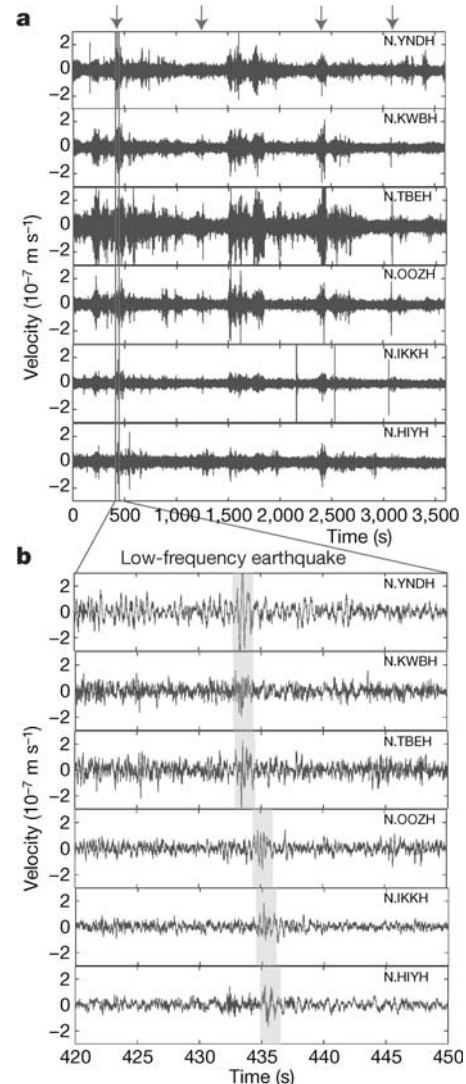


**Figure 2 | An extended period of tremor containing four identified LFEs.** **a**, One hour of unfiltered east component velocity seismograms for 29 August 2005, beginning at 17:00 local time during a tremor sequence as recorded at six Hi-net borehole stations (N.YNDH and so on) in western Shikoku. Arrows indicate times of LFEs. **b**, Expanded view of seismograms showing one LFE from **a**. S-wave arrivals can be identified on these seismograms between 433 s and 436 s and are highlighted in grey. Traces are ordered by the time of the S-wave arrival, with the earliest arrival on top. P-wave arrival is too weak to be obviously visible above the noise, even on vertical seismograms, but often can be measured for such events using cross-correlation.

(Supplementary Fig. S3). These correlations are especially important because they demonstrate similarity of the LFEs with known shear sources, and because they help locate the LFEs relative to intra-slab seismicity. The correlations with regular seismicity along with the observed larger S-wave amplitudes suggest that the LFEs themselves represent shear failure.

After relocation, the LFEs collapse onto a distinct plane 5–8 km above, and approximately parallel to, the dipping plane of seismicity within the subducting Philippine Sea slab (Fig. 4). In places, the plane of LFEs extends for nearly 20 km in the dip direction of the slab, with events strongly clustered along-strike (Fig. 3). Although it was previously thought that these events occurred within the overriding plate<sup>9</sup>, we believe they occur on the plate interface. This hypothesis is supported by an independent seismic refraction study, which finds that the plate interface is 3–5 km shallower than previous estimates<sup>16</sup>, with the top surface corresponding closely to our LFE locations.

Assuming average oceanic crustal thickness (8 km), the location of LFEs on the plate interface places the intra-slab seismicity primarily within the oceanic lower crust (Fig. 4d). An increase in P- and S-wave velocities seen just below the slab seismicity (Fig. 4), as well as recent receiver function analysis<sup>17</sup>, further support this location of the oceanic Moho. The intra-slab seismicity appears to begin within the lowermost crust at shallower depths, and to expand upward within the crust as the slab subducts. Such behaviour is consistent with thermal-petrologic models for this region, which predict metamorphic reactions to occur first within the hotter lower crust<sup>18</sup>, but contrasts with expectations that intra-slab seismicity occurs primarily within the upper crust<sup>19</sup>. This issue remains an important subject of future research.

In the immediate vicinity of the LFEs, we find a zone of high  $v_p/v_s$  ratio (1.9–1.95, where  $v_p$  and  $v_s$  are respectively P- and S-wave velocity), probably indicating high pore-fluid pressures<sup>20</sup>. Figure 4 shows the estimated P, S and  $v_p/v_s$  velocity structure on a cross-

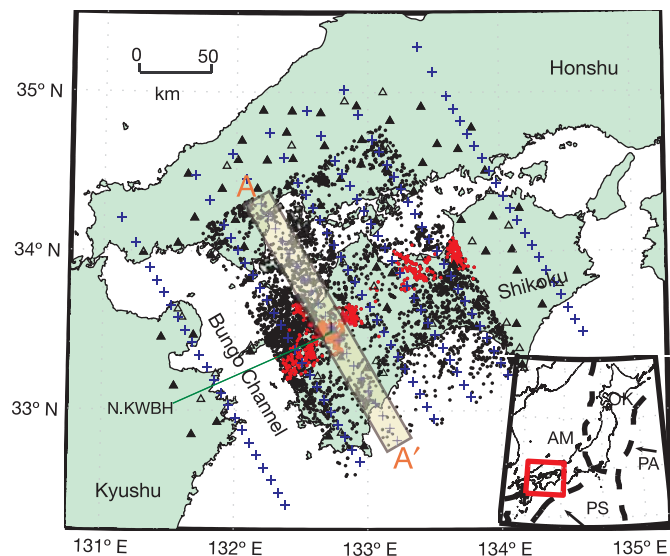


**Figure 3** | Area map with events, stations and velocity nodes used in the inversion. Black dots indicate regular earthquakes and red dots indicate LFEs. Open black triangles show seismic stations used in the inversion, filled black triangles denote Hi-net borehole stations, and blue plus signs indicate the horizontal locations of velocity nodes. The shaded yellow region shows the zone of earthquakes and LFEs plotted on cross-section A–A' in Fig. 4. Inset at lower right shows the broader tectonics of the region, with the red box indicating the area shown in the main figure. Dashed lines indicate plate boundaries. PA, Pacific plate; PS, Philippine Sea plate; AM, Amur plate; OK, Okhotsk plate. Plate model is PB2002<sup>20</sup>. Also shown is the location of station N.KWBH referred to in Supplementary Figs S1–S3.

section through an area of high LFE activity. A checkerboard test (Supplementary Fig. S4) demonstrates that our model is well resolved. The most prominent area of high  $v_p/v_s$  is located between the LFEs and the intra-slab seismicity, within the subducting crust. The high- $v_p/v_s$  zone is most pronounced on the cross-section with the most LFE activity (Fig. 4), and is consistent with the hypothesis that these LFEs are enabled by the release of fluids in the subduction zone. A likely source of fluids is dehydration of hydrous minerals within the subducting oceanic crust, a process also proposed to enable intra-slab seismicity<sup>19,21,22</sup>.

High pore-fluid pressure on the plate interface has the potential to alter the mode of slip by extending the conditionally stable region, as proposed for the Tokai segment at the northeast end of the Nankai trough<sup>23</sup> in order to explain a long-term slow slip event on this segment<sup>24</sup>. Interestingly, this region also experiences a high level of tremor activity<sup>1</sup>, with epicentral locations of the tremor matching a region of high  $v_p/v_s$  within the subducting crust<sup>23</sup>. This

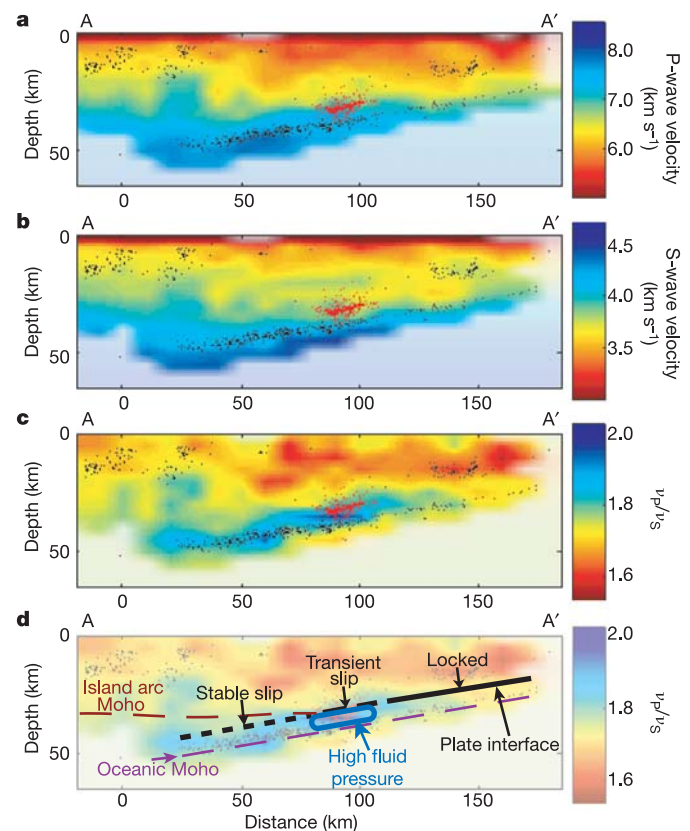


**Figure 4** | Seismic velocities and relocated hypocentres along cross-section A–A'. **a**, P-wave velocity,  $v_p$ . **b**, S-wave velocity,  $v_s$ . **c**,  $v_p/v_s$  ratio. This cross-section is selected because it cuts through the region of highest tremor and LFE activity (see Fig. 2). Relocated hypocentres are plotted for events within 9 km of the cross-section (the yellow highlighted region in Fig. 2), with black dots indicating regular earthquakes and the red dots indicating LFEs. Faded areas represent regions of poor resolution, where the derivative weight sum (DWS) value is less than 50. **d**, Schematic diagram of our interpretation overlaid on the  $v_p/v_s$  structure. We interpret the LFEs to occur on the plate interface, coincident with the zone of transient slip, while the seismicity within the slab occurs primarily within the oceanic lower crust. The oceanic Moho is drawn based on an 8 km crustal thickness, which is consistent with observed P- and S-wave velocities in **a** and **b**. Between the LFEs and slab seismicity, within the slab crust, is a distinct region of high  $v_p/v_s$  ratio (1.9–1.95), which we interpret as due to high fluid pressure. The plate interface updip of the LFEs is apparently locked, based on rupture models of the 1946 Nankai earthquake<sup>16,26</sup> and the lack of current seismicity. Downdip of the LFEs, the plate interface may slip stably. Also shown is the approximate location of the island arc Moho.

correspondence between active tremor and high  $v_p/v_s$  is strikingly similar to what we observe in western Shikoku.

Tremor has recently been discovered outside a subduction environment under the San Andreas fault system south of Parkfield<sup>25</sup>. This tremor, estimated to occur below the seismogenic zone at depths of 20–40 km, shares many characteristics with that observed in Japan and Cascadia. Like tremor in subduction zones, tremor on the San Andreas fault occurs in a region previously thought to deform aseismically, but no associated deformation transient has yet been detected.

We propose that the coupled phenomena of tremor, LFEs and episodic slow slip events represent a mode of failure for a transition zone between a locked and continuously creeping fault. In a subduction zone, this corresponds to the transition between the locked megathrust source region updip and the continuously slipping region downdip. In fact, models of co-seismic rupture for the 1946  $M_w$  (moment magnitude) 8.2 Nankai earthquake<sup>16,26</sup> terminate only a short distance updip of the observed band of LFEs. Some areas where tremor and LFEs occur, such as the Tokai (discussed above) and Bungo Channel regions, have also been observed to fail in longer duration slow slip events<sup>24,27,28</sup>, demonstrating a tendency for transient slip in these areas.

Precise locations indicate that the LFEs analysed in this study occur on the plate interface. The correlation between LFEs and regular seismicity, the fact that LFEs are primarily composed of shear waves, and the remarkable correspondence with slow slip events<sup>5–7</sup> argue that LFEs represent shear slip on this interface. We propose that LFEs may be generated by local slip accelerations at geometric or frictional heterogeneities that accompany large slow slip events on the plate interface. Long-duration tremor may result simply from a superposition of many concurrent LFEs. Alternatively, long-duration tremor might represent a combined signal of shear slip and fluid flow. We hypothesize that increasing fluid pressure may reduce the effective normal stress and enable slip on the plate interface; this slip could increase permeability and allow pressurized fluid to escape, possibly contributing to the tremor signal in the process. In either case, evidence discussed above suggests that fluids play a key role in the failure process. Remote triggering of tremor and LFEs<sup>29</sup>, reminiscent of earthquake triggering seen in hydrothermal regions, provides additional evidence for fluid enablement.

As noted by previous authors<sup>2,27</sup>, a slow slip event on the subduction interface would increase the stress updip on the locked portion, potentially elevating the probability of a large earthquake during or soon after the slow slip. The same concept applies to other fault settings with juxtaposed locked and creeping portions, like the San Andreas<sup>25</sup>. If LFEs are direct signals of episodic slow slip, they would illuminate aseismic slip at depth with temporal and spatial precision well beyond that attainable with surface geodetic instruments. With proper instrumentation and analysis, we will probably detect similar events within tremor in regions beyond southwest Japan. Consequently, LFEs may provide critical information for monitoring the seismic hazard in a variety of tectonic settings.

Received 17 January; accepted 18 May 2006.

1. Obara, K. Nonvolcanic deep tremor associated with subduction in southwest Japan. *Science* **296**, 1679–1681 (2002).
2. Rogers, G. & Dragert, H. Episodic tremor and slip on the Cascadia subduction zone: The chatter of silent slip. *Science* **300**, 1942–1943 (2003).
3. Dragert, H., Wang, K. & James, T. S. A silent slip event on the deeper Cascadia subduction interface. *Science* **292**, 1525–1528 (2001).
4. Miller, M. M., Melbourne, T., Johnson, D. J. & Sumner, W. Q. Periodic slow earthquakes from the Cascadia subduction zone. *Science* **295**, 2423 (2002).
5. Obara, K., Hirose, H., Yamamizu, F. & Kasahara, K. Episodic slow slip events accompanied by non-volcanic tremors in southwest Japan subduction zone. *Geophys. Res. Lett.* **31**, doi:10.1029/2004GL020848 (2004).
6. Hirose, H. & Obara, K. Repeating short- and long-term slow slip events with deep tremor activity around the Bungo channel region, southwest Japan. *Earth Planets Space* **57**, 961–972 (2005).

7. Obara, K. & Hirose, H. Non-volcanic deep low-frequency tremors accompanying slow slips in the southwest Japan subduction zone. *Tectonophysics* **417**, 33–51 (2006).
8. Seno, T. & Yamasaki, T. Low-frequency tremors, intraslab and interplate earthquakes in Southwest Japan—from a viewpoint of slab dehydration. *Geophys. Res. Lett.* **30**, doi:10.1029/2003GL018349 (2003).
9. Katsumata, A. & Kamaya, N. Low-frequency continuous tremor around the Moho discontinuity away from volcanoes in the southwest Japan. *Geophys. Res. Lett.* **30**, doi:10.1029/2002GL015981 (2003).
10. Chouet, B. Resonance of a fluid-driven crack: Radiation properties and implications for the source of long-period events and harmonic tremor. *J. Geophys. Res.* **93**, 4375–4400 (1988).
11. Julian, B. R. Volcanic tremor: Nonlinear excitation by fluid flow. *J. Geophys. Res.* **99**, 11859–11878 (1994).
12. Kao, H. *et al.* A wide depth distribution of seismic tremors along the northern Cascadia margin. *Nature* **436**, 841–844 (2005).
13. Zhang, H. & Thurber, C. H. Double-difference tomography: The method and its application to the Hayward fault, California. *Bull. Seismol. Soc. Am.* **93**, 1875–1889 (2003).
14. Zhang, H. *et al.* High-resolution subducting-slab structure beneath northern Honshu, Japan, revealed by double-difference tomography. *Geology* **32**, 361–364 (2004).
15. Obara, K., Kasahara, K., Hori, S. & Okada, Y. A densely distributed high-sensitivity seismograph network in Japan: Hi-net by National Research Institute for Earth Science and Disaster Prevention. *Rev. Sci. Instrum.* **76**, doi:10.1063/1.1854197 (2005).
16. Baba, T., Tanioka, Y., Cummins, P. & Uhira, K. The slip distribution of the 1946 Nankai earthquake estimated from tsunami inversion using a new plate model. *Phys. Earth Planet. Inter.* **132**, 59–73 (2002).
17. Shiomi, K., Sato, H., Obara, K. & Ohtake, M. Configuration of subducting Philippine Sea plate beneath southwest Japan revealed from receiver function analysis based on the multivariate autoregressive model. *J. Geophys. Res.* **109**, doi:10.1029/2003JB002774 (2004).
18. Peacock, S. M. & Wang, K. Seismic consequences of warm versus cool subduction metamorphism: Examples from southwest and northeast Japan. *Science* **286**, 937–939 (1999).
19. Hacker, B. R., Peacock, S. M., Abers, G. A. & Holloway, S. D. Subduction Factory 2. Are intermediate-depth earthquakes in subducting slabs linked to metamorphic dehydration reactions? *J. Geophys. Res.* **108**, doi:10.1029/2001JB001129 (2003).
20. Christensen, N. I. Pore pressure and oceanic crustal seismic structure. *Geophys. J. R. Astron. Soc.* **79**, 411–423 (1984).
21. Raleigh, C. B. & Paterson, M. S. Experimental deformation of serpentinite and its tectonic implications. *J. Geophys. Res.* **70**, 3965–3985 (1965).
22. Kirby, S. H. Intraslab earthquakes and phase changes in subducting lithosphere. *Rev. Geophys.* **33**, 287–297 (1995).
23. Kodaira, S. *et al.* High pore fluid pressure may cause silent slip in the Nankai Trough. *Science* **304**, 1295–1298 (2004).
24. Ozawa, S. *et al.* Detection and monitoring of ongoing aseismic slip in the Tokai region, central Japan. *Science* **298**, 1009–1012 (2002); published online 3 October 2002 (doi:10.1126/science.1076780).
25. Nadeau, R. M. & Dolenc, D. Nonvolcanic tremors deep beneath the San Andreas fault. *Science* **307**, 389 (2005); published online 9 December 2004 (doi:10.1126/science.1107142).
26. Tanioka, Y. & Satake, K. Coseismic slip distribution of the 1946 Nankai earthquake and aseismic slips caused by the earthquake. *Earth Planets Space* **53**, 235–241 (2001).
27. Hirose, H., Hirahara, K., Kimata, F., Fujii, N. & Miyazaki, S. A slow thrust slip event following the two 1996 Hyuganada earthquakes beneath the Bungo Channel, southwest Japan. *Geophys. Res. Lett.* **26**, 3237–3240 (1999).
28. Miyazaki, S., McGuire, J. J. & Segall, P. A transient subduction zone slip episode in southwest Japan observed by the nationwide GPS array. *J. Geophys. Res.* **108**, doi:10.129/2001JB000456 (2003).
29. Miyazawa, M. & Mori, J. Detection of triggered deep low-frequency events from the 2003 Tokachi-oki earthquake. *Geophys. Res. Lett.* **32**, doi:10.1029/2005GL022539 (2005).
30. Bird, P. An updated digital model of plate boundaries. *Geochem. Geophys. Geosyst.* **4**, doi:10.1029/2001GC000252 (2003).

**Supplementary Information** is linked to the online version of the paper at [www.nature.com/nature](http://www.nature.com/nature).

**Acknowledgements** This material is based upon work supported by the National Science Foundation. We thank K. Obara for allowing us to use his determinations of daily tremor activity. Much of this work was conducted while D.R.S. was a participant in the Summer Institute in Japan programme, cosponsored by the Japan Society for Promotion of Science and the National Science Foundation. All data were obtained from the NIED Hi-net data server.

**Author Information** Reprints and permissions information is available at [ngp.nature.com/reprintsandpermissions](http://ngp.nature.com/reprintsandpermissions). The authors declare no competing financial interests. Correspondence and requests for materials should be addressed to D.R.S. ([dshelly@pangea.stanford.edu](mailto:dshelly@pangea.stanford.edu)).